Measurement of the $\Lambda/\bar{\Lambda}$ particles in Au+Au at $\sqrt{s_{NN}} = 200$ GeV

Part 1: Hadron Identification in EMC (PbSc)

A. Taranenko , N.N. Ajitanand, J. Alexander, W. G. Holzmann,
M. Issah, R. A. Lacey, P. Chung

Department of Chemistry, State University of New-York at Stony Brook

Draft 1. July 09, 2003

1 Abstract

The purpose of this analysis note is to study the timing resolution of EMC (PbSc) for hadrons and to write the code for probability functions isPi, isK and isP which define the number of sigmas by which the square of mass of the track deviates from the assumption that this track itself is pion, kaon, proton. These functions should take into account the different timing response of calorimeter on particle type, deposited energy and momentum of the particle.

2 Hadron identification in Phenix

In Phenix experiment the hadron identification is based on simultaneous measurements of the particle's momentum **p** (measured by Drift Chamber) and time-of-flight **tof** (measured by high resolution TOF detector or Electromagnetic Calorimeter and BBC). The particle identification (PID) technique is well developed for TOF detector , see [6, 7], and user can select pions, kaons and protons using the probability functions isPi, isK and isP from the utiHadPiD utility library [8] which give us number of sigmas by which the measured mass square m^2_{meas} of the track deviates from the presumption that the track itself is pion, kaon, proton. For example $|isPi|$ <2 means $|m^2_{meas} - m^2_{centroid}(pion)| < 2\sigma_{m^2}$, where the $m^2_{centroid}$ is the centroid position of the mass-squared distribution peak for pion and σ_{m^2} is the width of the mass squared peak (m^2 resolution). In reality the measured centroid position of the m^2 distributions for pion, kaon and proton can be different from the values from the Particle Data Book and their values are momentum dependent. In case of TOF detector the momentum dependence of the centroid position of m^2 distribution can be removed by applying the constant global TOF offset and the difference from the Particle Data Book by correcting the momentum scale as described in [7, 9].
The width of m^2 peak (m^2 resolution) is dependent on both the momentum resolution σ_p of the Drift Chamber and timing resolution of σ_{tof} of TOF detector. The total momentum resolution σ_p is the combination of the intrinsic angular resolution of the Drift Chamber σ_α and the angular displacement σ_{ms} caused by mupliple scattering of a charged particle with the materials up to the Drift Chamber [7]. The timing resolution for hadrons can be estimated by measuring the width of the difference between the measured time of flight and the expected time of flight for high momentum pions, see Fig.1.

The expected flight time for pion was calculated from the path length following particle trajectory from vertex to EMC (L), momentum (p) and mass of pion (m_π) in the following way:

$$t_{expected} = \frac{L}{c}\sqrt{1 + \left(\frac{m_\pi c}{p}\right)^2}, \tag{1}$$

This method gives the value $\sigma_{tof} \simeq$ 120-130 ps for TOF detector and it was found to be independent on momentum of particle, see [9].
Therefore, in case of TOF detector the values for the resolutions (σ_α, σ_{ms}, σ_{tof}) can be determined using a simultaneous three parameter fit to the sigma values of the measured m^2 distributions as a function of momenta for pions, kaons and protons. The following parametrization can be used for this fit, see [7]:

$$\sigma^2_{m^2} = \frac{\sigma^2_{\alpha^2}}{K^2_1}(4m^4p^2) + \frac{\sigma^2_{ms}}{K^2_1}[4m^4(1 + \frac{m^2}{p^2})] + \frac{\sigma^2_{tof}c^2}{L^2}4p^2(m^2 + p^2) \tag{2}$$

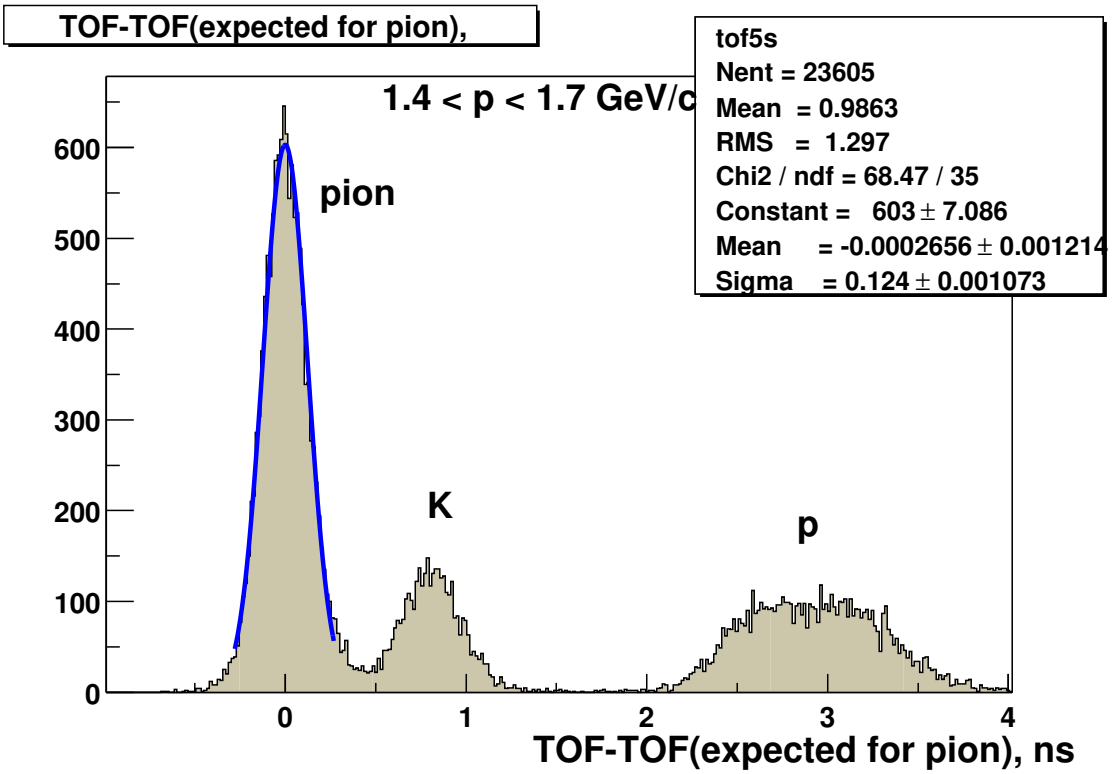

Figure 1: The difference of the measured and expected time for pions with momentum ($1.4 \leq p \leq 1.7$ GeV/c) for TOF detector

If $m^2_{centroid}$ and m^2 resolution determined correctly the n-sigma PID distributions isPi, isK and isP should be centered at zero and have 1-sigma width of one independent of momentum of particle, charge, centrality etc.

In order to build the PID functions for hadrons detected in EMC we need to know the timing resolution of PbSc for hadrons (this give us m^2 resolution) and we need to apply the corrections for T0 offset in order to make the position of $m^2_{centroid}$ close to the Particle Data Book value for each particle.

3 Timing resolution and T0 offset for hadrons in EMC

What do we know about EMC timing ?

- EMCal timing information comes only from the central tower of EMC cluster, see [4]
- By convention the EMC timing in microDST-v03 is calibrated to have a peak at zero for photons, everywhere in the calorimeter, and independent of the vertex. This done by subtracting the "photon flash" time T_{flash} (time for a v=c particle along a straight line from the measured vertex) from the time of emc cluster:
  T_{flash}=dist/c = $\sqrt{Xemc^2 + Yemc^2 + (Zemc - Zvtx)^2}/c$, where
  Xemc, Yemc, Zemc - coordinates of the emc cluster and Zvtx - measured vertex.
  In CNT-nDST's the EMC time-of-flight has been corrected by adding "photon flash" time back, which make it more useful for calculating the properties of hadrons.

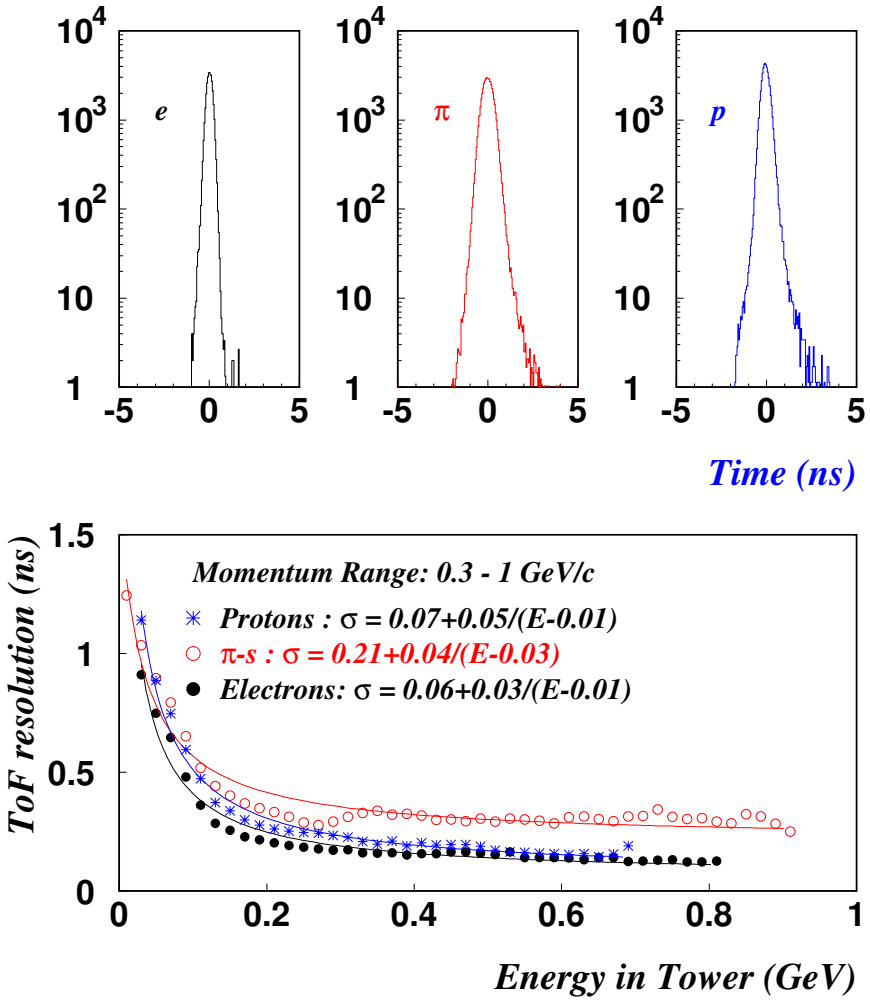

Figure 2: EMC PbSc timing resolution as a function of the energy deposited in the central tower for different particles in the momentum range 0.3-1 GeV/c from the beam test data. Figure is taken from [12].

- We know that after the " global (run independent) tower by tower corrections and sector-wide run by run corrections performed by the EMC group using the clear sample of photons and applied in the first afterburner, the time of flight peak for photons (T0 offset) is generally withing 100 ps from zero and has sigma (timing resolution) around or better $\sigma_{tof} \simeq 400$ ps", see [13].

- In contrast to the TOF detector the timing resolution of EMC is not constant - it depends on energy deposited in the central tower of the cluster, momentum of particle, particle type, charge, , incident angle of the track etc, see [10, 11, 13]. As example, Fig.2 shows the dependence of timing resolution of EMC (PbSc) as a function of energy deposited in the central tower of the cluster for different particle from the beam test, see [12]. For very low deposited energies the timing resolution can be as bad as σ_{tof} ≃1-1.2 ns and at deposited energies >0.2 GeV it becomes nearly constant (100 ps for electrons and 200 ps for hadrons). The explanation of such behaviour of σ_{tof} EMC can be found in [10, 11, 12, 13]. We can estimate the σ_{tof} EMC for hadrons using the sigma of

the distribution **temc**-time(expected for pions), as it was done in case of TOF detector, see [9] and Eq.1. Fig.3 shows the dependence of the timing resolution of EMC (PbSc) as a function of energy deposited in the central tower of the cluster for charged pions measured in W0-W2 sectors of EMC for AuAu data. The shape of the dependence σ_{tof} vs **Ecent** for charged pions looks the same as in the beam test, it is nearly constant at deposited energies >0.2 GeV. However the timing resolution in the beam test data almost two times better than in AuAu run were $\sigma_{tof} \simeq 400$ ps for Ecent > 0.2 GeV.

- Slewing effect (i.e. an energy dependent readout of TDC), variation of depth of EMCal showers, cross talk of adjacent channels in EMC electronics , inclined tracks ,.. etc , see [10, 11, 13] can lead to shifts in the absolute time (T0 offset) → shift in the position of mass^2 peak. This shift may provide a dependence on species (and sign). The correction for the timing shift may be complex in contrast to the TOF detector , were the one global run-dependent T0 offset was enough to make the position of mass^2 peak close to the Particle Data Book value.

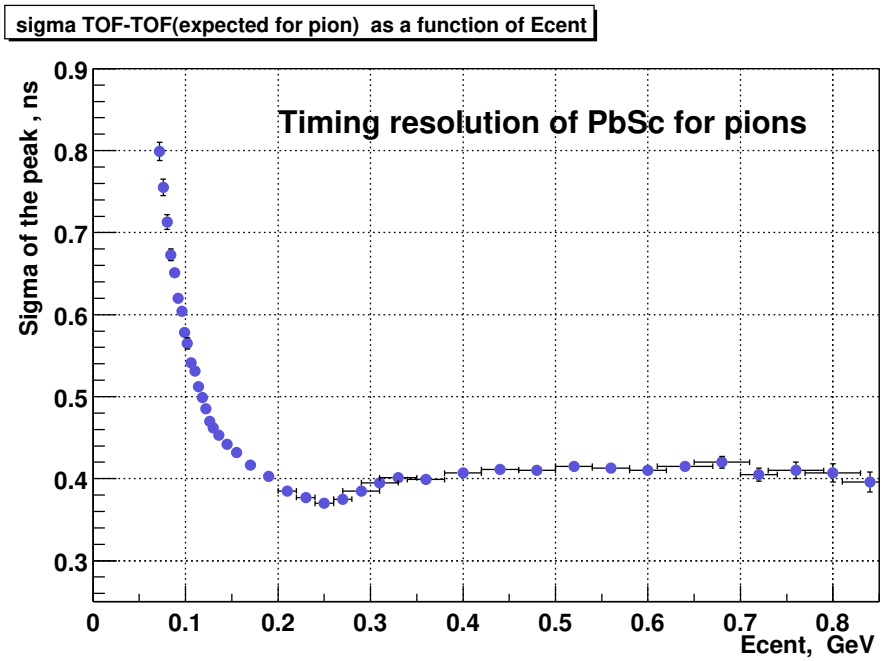

Figure 3: EMC PbSc timing resolution for charged pions with momentum 0.6≤ p ≤ 0.8 GeV/c as a function of the energy deposited in the central tower of the cluster for sectors W0-W2.

The fact that the timing resolution of PbSc is not constant makes difficulties in using fit by Eq.2 for extraction the values of mass^2 resolution σ_{mass^2}. In order to overcome this problem we will use the reasonable polynomial fit for the momentum dependence of mass^2 resolution for each particle species and charge separately. But, before it we need to correct the EMC T0 offset in order to make the position of mass^2 close to the Particle Data Book value for each particle. We will define the T0 offset as the position of the peak **temc**-time(expected for each particle). As the correction for T0 offset in EMC is complex we will study it as a function of momentum , particle type, sign and the energy deposited in the central tower of the cluster **Ecent**. As an example Fig.4 shows the **Ecent** dependence of T0 offset for pions.

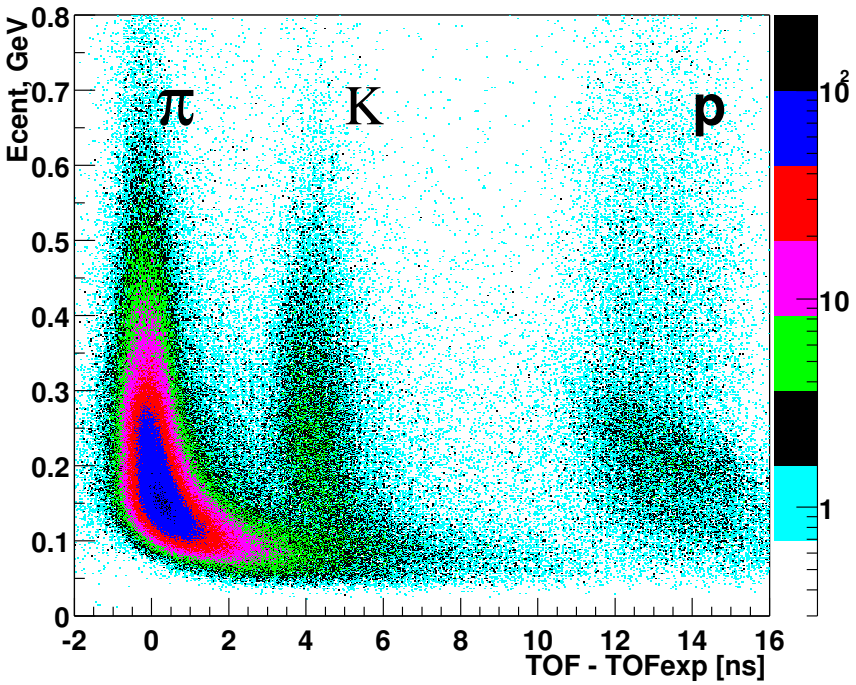

Figure 4: The difference of the measured and expected time for pions with momentum (0.6 $\leq$ p $\leq$ 0.7 GeV/c) as a function of energy in the central tower of the cluster Ecent (East Arm , sectors E2+E3)

4 Data sample and event selection

In our analysis of PID for hadrons detected by East Arm PbSc we used the "afterburner" version of v03 Central Track (CNT) nanoDST's.
The only full field runs (after 27808) are used. The following runs were excluded:

- Photon converter runs and reverse field runs
- runs from the list: MOM.txt [3] (mean momentum of DC tracks are outside of 0.55 to 0.65 GeV/c range)
- runs from the list: NDC.txt [3] (number of DC tracks are outside range)
- bad PC1 runs (32010-32441)
- runs with number of segments less than 10 were excluded

The analysis is restricted to events fulfilling the following conditions:
1) Minimum bias events (TriggerHelper::IsEventMinBias()==true)
2) BBC vertex cut: $|z_{BBC}| \leq 30$ *cm*.
3) centrality cut: 0 <centrality (by clock method)$\leq$ 92.
Track selection
The following single track cuts were used:
DCH:

1) Dch quality cut: 31 and 63 only.

2) Dch Zed cut: $|Zed| < 75$ cm (to limit the edge effect)

Matching cuts:

1) 2.0 sigma EMC&&PC3 momentum dependent radial matching cuts

EMC:

1) sectors E2 and E3 only (PbSc)

2) EMC timing **temc** cut: temc < 60 ns - remove junk because of overflow in the TDC-s [16]

3) (warnmap & 0x02000000)==0 - there is no time-of-flight "problems" in the central tower of the cluster (EMCal timing information comes only from the central tower of the EMC cluster), see [4]

5 T0 offset determination

5.1 Run and sector dependence of T0

We found that in **momentum-Ecent** range (0.7≤ p ≤0.8 GeV/c and 0.2≤E_{cent} ≤0.25 GeV) the T0 offset for charged pions is almost independent on **Ecent** and momentum, but it is slightly dependent on selected run number and EMC sector. First we will determine and remove this residual sector-run dependence in T0 by plotting temc-time(expected for pions) in this **momentum-Ecent** range and applying the correction in order to put the postion of the peak to zero **temc=temc+T0(run, sector)**, as it is shown in Fig.5 and Fig.6. The resulting corrections are plotted in Fig.7 as a function of the run number for sectors E2 (blue points) and E3 (red points).

5.2 Ecent dependence of T0 - "slewing correction"

After removing the residual sector-run dependence in T0 , we used the sample of ≃ 9 M minimum bias events to study the **Ecent** dependence of T0 offset for each particle and sign.

Pions: Fig.8 shows the dependence of T0 offset (centroid of the difference temc-time(expected for π^+)) as a function of E_{cent} for different bins in momentum of π^+ detected in sector E3. E_{cent} dependence of T0 offset for pions looks to be universal and can be fitted by one functional if a constant T0 offset will be added for low momentum pions as it is shown in Fig. 9. There is no big difference in **Ecent** dependence of T0 offset for sector E2 and E3 was found, see the comparison of Fig. 9 (E3) and Fig.10 (E2) for π^+ and Fig.11 (E2) and Fig.12 (E3) for π^- mesons. There is a difference in **Ecent** dependence for positive and negative pions was found , see Fig. 10 (E2, π^+) and Fig.11 (E2, π^-) for comparison.

Kaons: E_{cent} dependence of T0 offset for kaons is presented in Fig.13-14 for K^- and in Fig.15-16 for K^+. From these plots we can draw nearly the same conclusions as for pions: there is no big difference between sectors and studied bins in momentum of kaons, but the difference exists between K^- and K^+.

Protons: Fig.17 - 18 shows the E_{cent} dependence of T0 offset for protons and anti-protons respectively. The conclusions are roughly the same , exluding that for anti-protons we used different parametrization for low and high momentum, see Fig.18.

The energy dependent shifts in EMC PbSc timing peak were studied also by S. Mioduszewski using the photon event sample, see [15]. The universal correction factor for T0 offset was found to be: $0.19(\ln(\text{Ecent})+0.74)^2$ and it was applyed in the afterburner process for EMC timing with condition

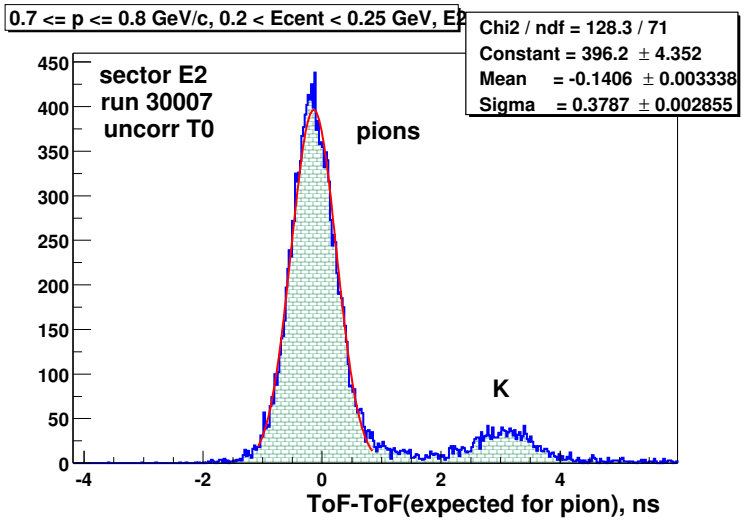

Figure 5: The run dependence of T0 offset (centroid of the difference temc-time(expected for π) for 0.7$\leq$ p $\leq$0.8 GeV/c and 0.2$\leq$E$_{cent}$ $\leq$0.25 GeV) for sectors E2 and E3

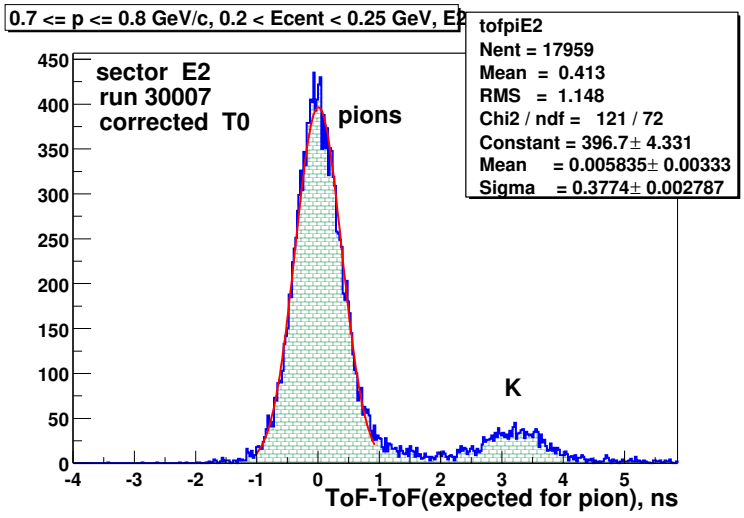

Figure 6: The run dependence of T0 offset (centroid of the difference temc-time(expected for π) for 0.7$\leq$ p $\leq$0.8 GeV/c and 0.2$\leq$E$_{cent}$ $\leq$0.25 GeV) for sectors E2 and E3

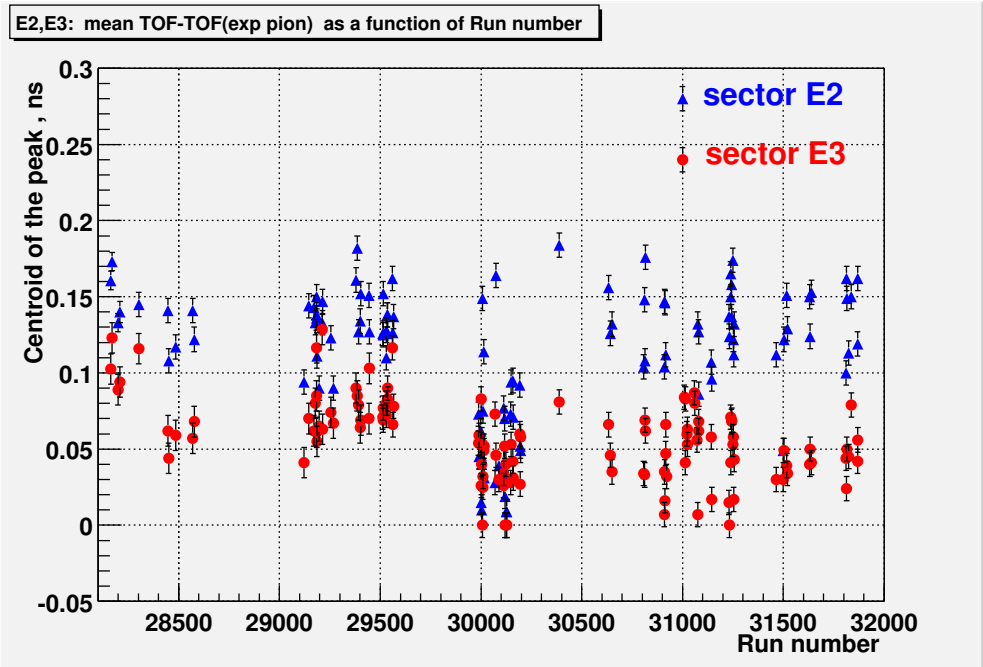

Figure 7: The run dependence of T0 offset (centroid of the difference temc-time(expected for π) for 0.7$\leq$ p $\leq$0.8 GeV/c and 0.2$\leq$E$_{cent}$ $\leq$0.25 GeV) for sectors E2 and E3

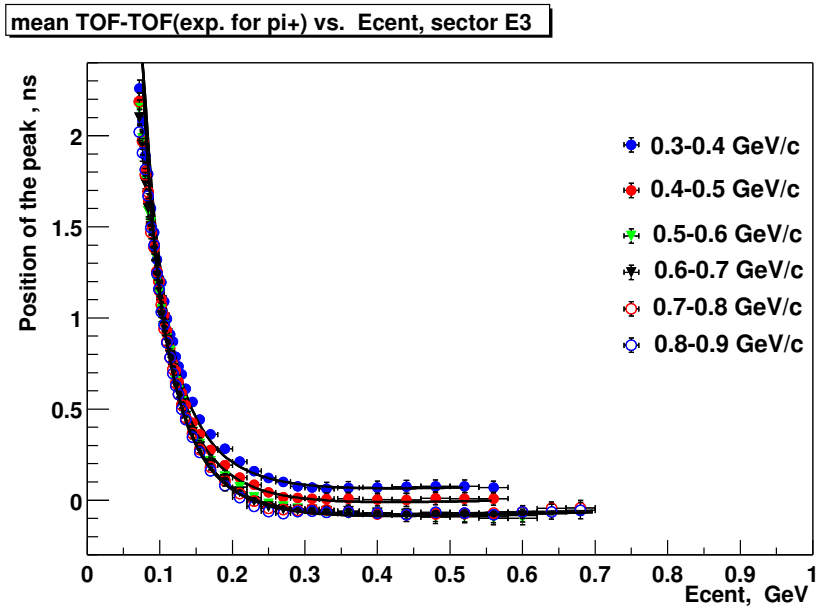

Figure 8: T0 offset (centroid of the difference temc-time(expected for π^+) as a function of E$_{cent}$ for different bins in momentum of π^+ detected in sector E3.

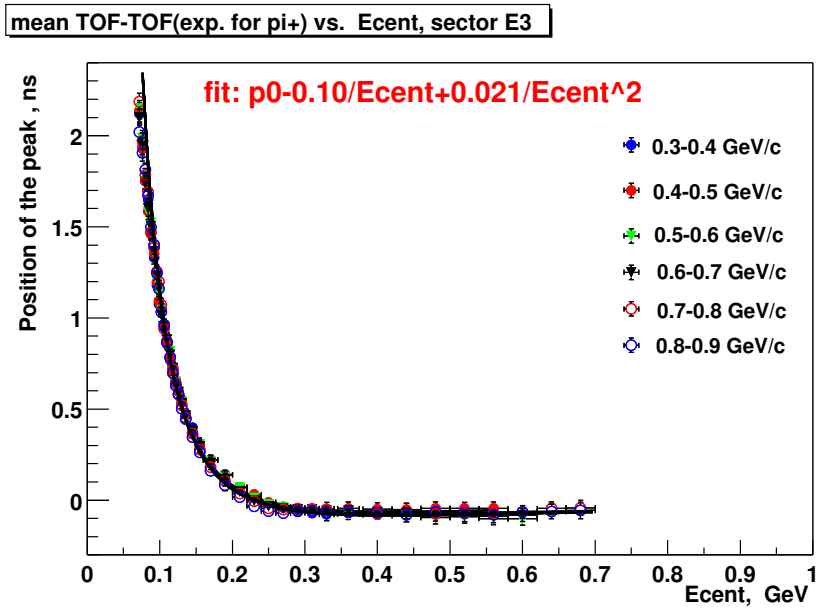

Figure 9: T0 offset (centroid of the difference temc-time(expected for π^+) as a function of E_{cent} for different bins in momentum of π^+ detected in sector E3. A constant T0 offset was added for low momentum pions In order to show that the E_{cent} dependence of T0 offset looks to be universal and can be fitted by one functional.

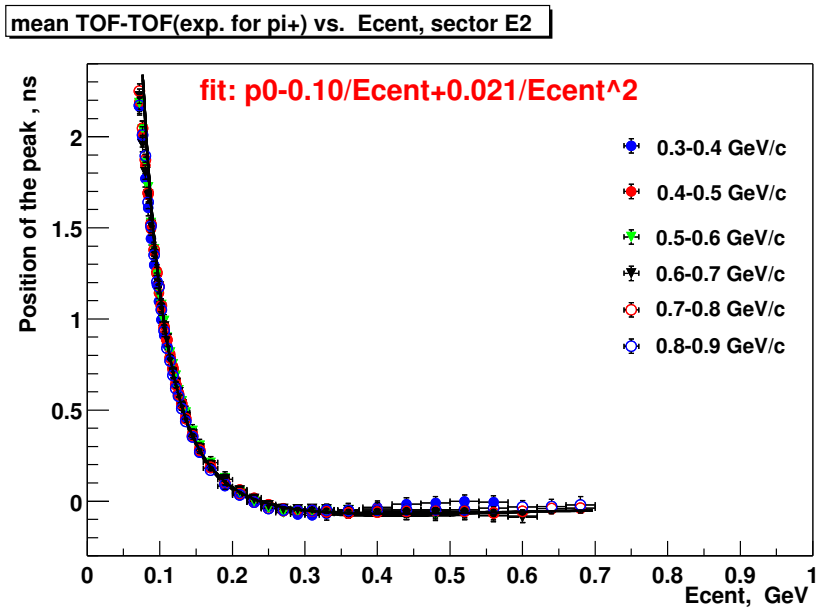

Figure 10: T0 offset (centroid of the difference temc-time(expected for π^+) as a function of E_{cent} for different bins in momentum of π^+ detected in sector E2. A constant T0 offset was added for low momentum pions In order to show that the E_{cent} dependence of T0 offset looks to be universal and can be fitted by one functional.

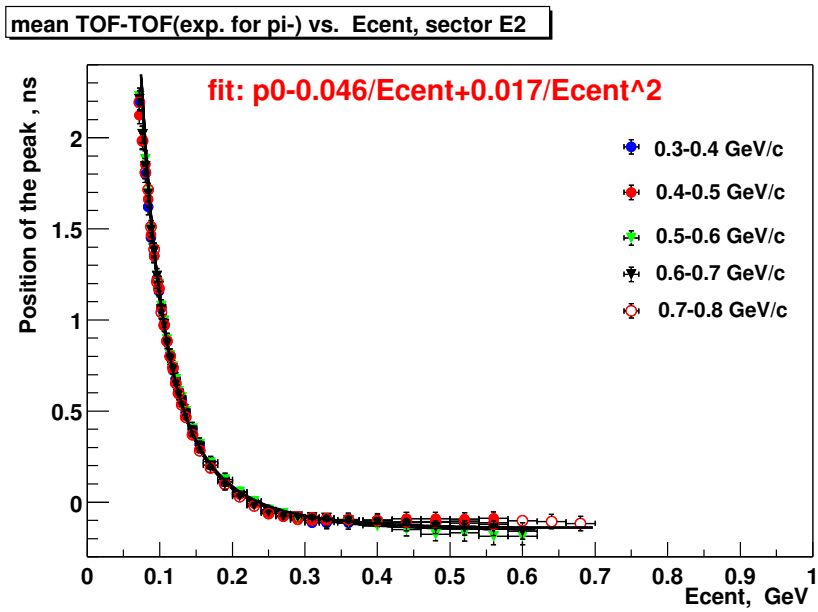

Figure 11: T0 offset (centroid of the difference temc-time(expected for π^-) as a function of E_{cent} for different bins in momentum of π^- detected in sector E2. A constant T0 offset was added for low momentum pions In order to show that the E_{cent} dependence of T0 offset looks to be universal and can be fitted by one functional.

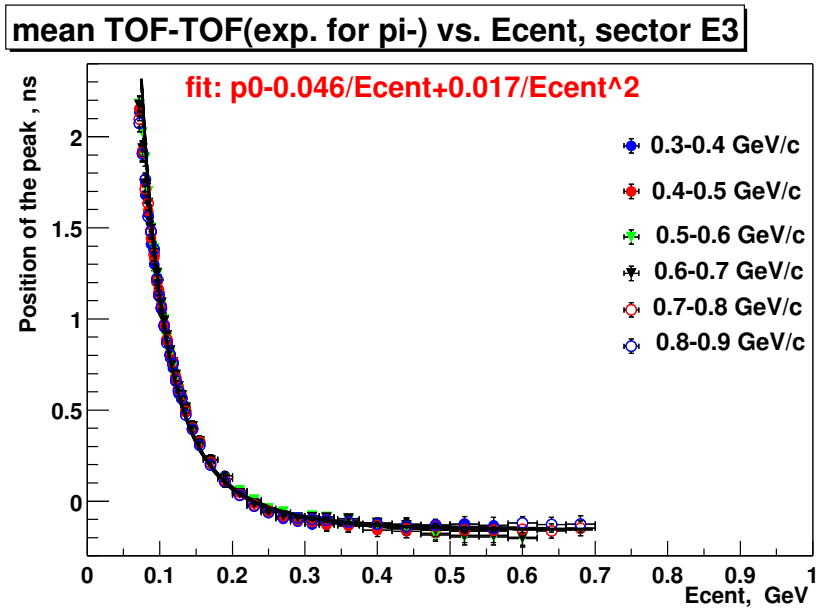

Figure 12: T0 offset (centroid of the difference temc-time(expected for π^-) as a function of E_{cent} for different bins in momentum of π^- detected in sector E3. A constant T0 offset was added for low momentum pions In order to show that the E_{cent} dependence of T0 offset looks to be universal and can be fitted by one functional.

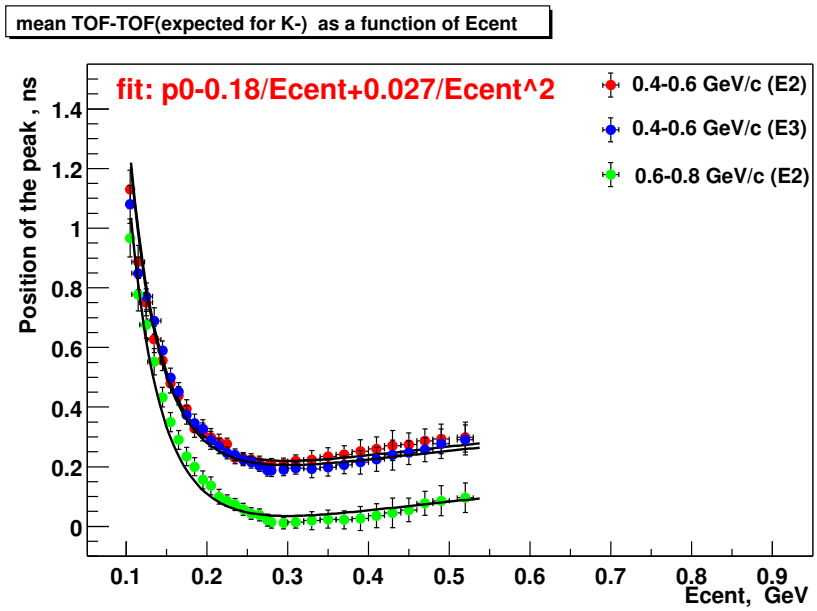

Figure 13: T0 offset (centroid of the difference temc-time(expected for K^-) as a function of E_{cent} for K^- in detected in sectors E2 and E3 for two momentum bins 0.4-0.6 GeV/c and 0.6-0.8 GeV/c.

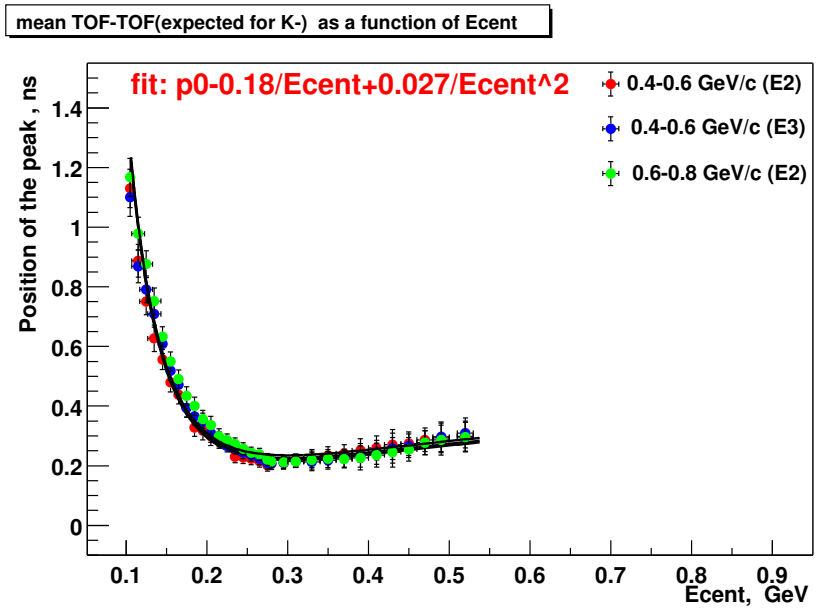

Figure 14: T0 offset (centroid of the difference temc-time(expected for K^-) as a function of E_{cent} for K^- in detected in sectors E2 and E3 for two momentum bins 0.4-0.6 GeV/c and 0.6-0.8 GeV/c , a constant T0 offset was added for 0.6-0.8 GeV/c bin

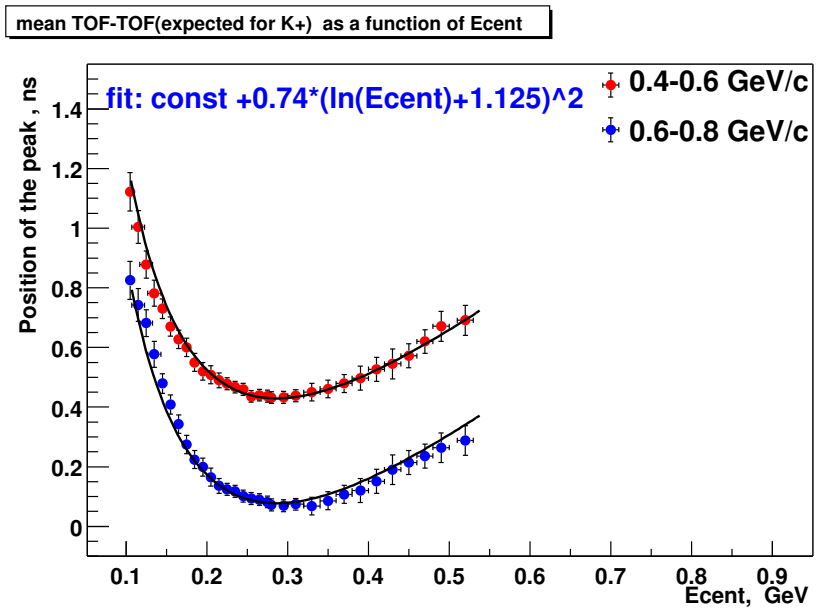

Figure 15: T0 offset (centroid of the difference temc-time(expected for K^+) as a function of E_{cent} for K^+ detected in sectors E2 and E3 for two momentum bins 0.4-0.6 GeV/c and 0.6-0.8 GeV/c.

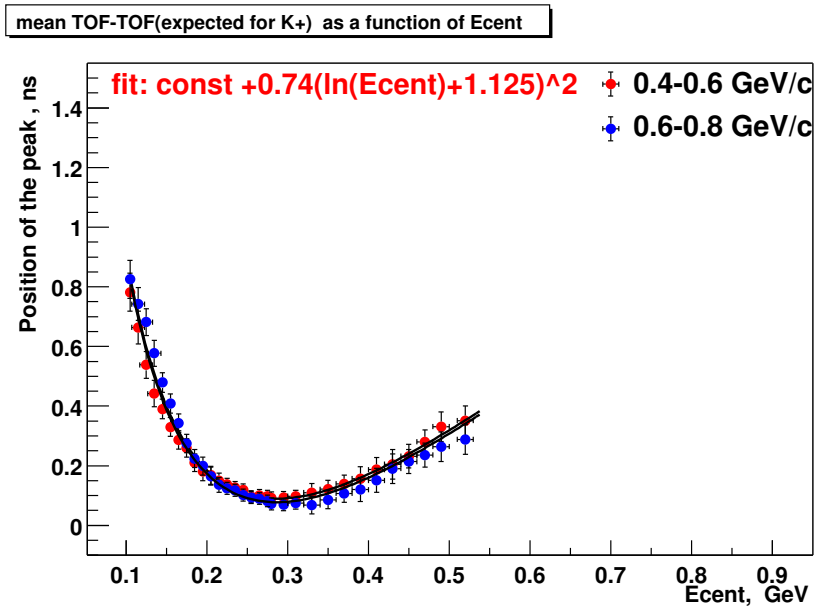

Figure 16: T0 offset (centroid of the difference temc-time(expected for K^+) as a function of E_{cent} for K^+ detected in sectors E2 and E3 for two momentum bins 0.4-0.6 GeV/c and 0.6-0.8 GeV/c , a constant T0 offset was added for 0.4-0.6 GeV/c bin

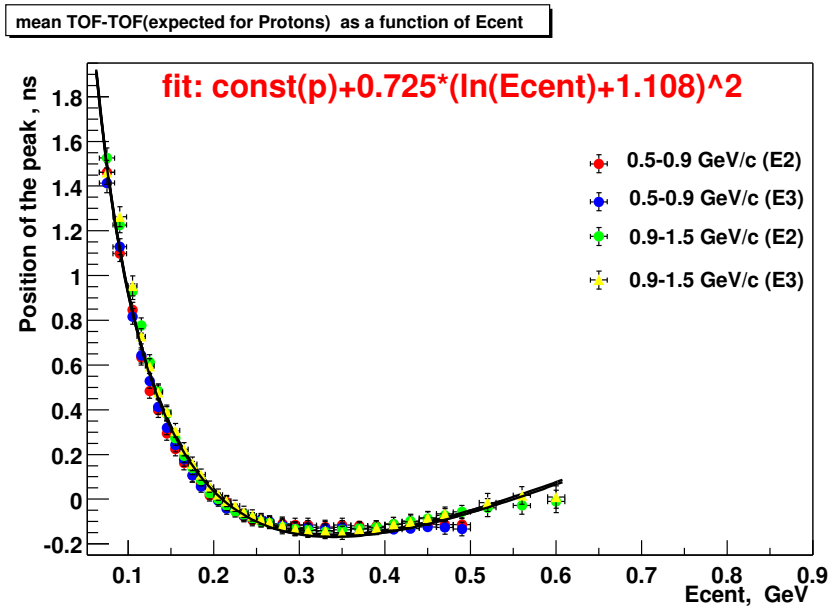

Figure 17: T0 offset (centroid of the difference temc-time(expected for protons) as a function of E_{cent} for two bins in momentum of proton. detected in sectors E2 and E3. T0 offset for low momentum protons shifted by a constant in order to fit the dependence at high momentum

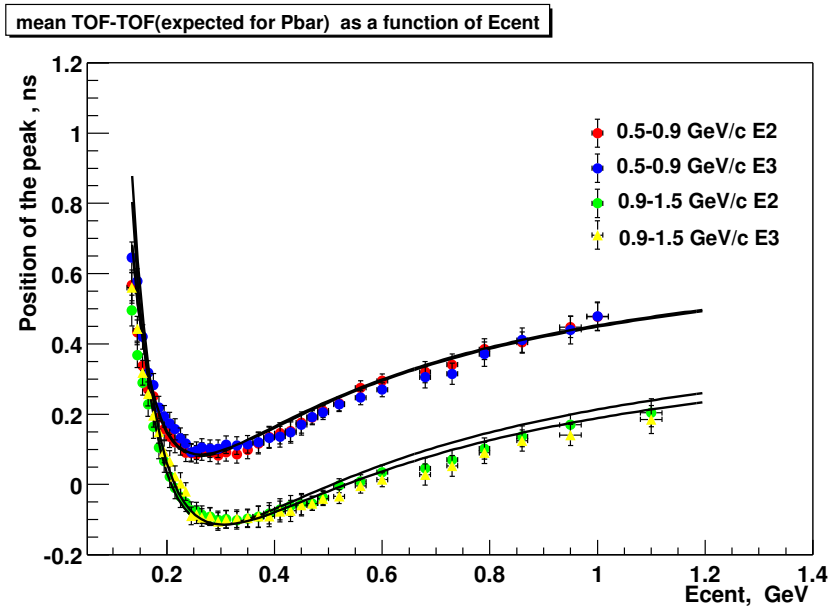

Figure 18: T0 offset (centroid of the difference temc-time(expected for $\bar{p}$) as a function of E_{cent} for two bins in momentum of anti-protons detected in sectors E2 and E3.

Ecent > 1 GeV. This condition for Ecent should affect the EMC timing for hadrons as the typical range of **Ecent** for hadrons is less than 1 GeV.

5.3 Momentum dependence of T0 offset

After removing the **Ecent** dependence in T0 offset for each particle species we will study the momentum dependence of T0.

Pions: Fig. 19 - 20 and Fig.21-22 show the momentum dependence of T0 offset for positive and negative pions respectively. T0 offset as a function of momentum is almost constant after 0.5 GeV/c. The momentum dependence of T0 offset is slightly different for different EMC sectors and charge of the particle, see Fig. 19-22. After removing the residual momentum dependence in T0 offset, we will receive the position of mass^2 peak for pions close to the Particle Data Book value, see Fig. 23-24.

Kaons: Fig. 25-26 show the momentum dependence of T0 offset for positive and negative kaons respectively. The difference between positive and negative kaons is more significant than in case of pions especially for low momentum kaons. In order to describe the momentum (**mom**) dependece of T0 offset we used the fit by the following functions: p0+p1/mom for kaon momentum <0.6 GeV/c and p0+p1/mom+p2/mom^2 for kaon momentum > 0.6 GeV/c. The resulting plots for momentum dependence of the position of mass^2 peak for positive and negative kaons are plotted in Fig. 27-28 respectively. The distributions are flat as a function of momentum and the positions of mass^2 peak for K^+ and K^- are close to the Particle Data Book value.

Protons and antiprotons: The momentum dependence of T0 offset for protons and $\bar{p}$ is more complex , see Fig.29-30. Here, in order to remove the momentum dependence we divided the whole momentum range into three bins and used the polynominal fit for each bin separately. The resulting distributions of the position of mass^2 peak after applying all corrections are plotted in Fig.31 for protons and Fig.32 for $\bar{p}$ respectively.

5.4 Momentum dependence of Mass^2 resolution for hadrons

We determined the corrections for T0 offset in order to make the position of $m^2_{centroid}$ close to the Particle Data Book value for each particle. Now we will determine the sigma of mass^2 peak (σ_{m^2} resolution) for each particle as a function of the momentum. For each bin in momentum will plotted mass^2 distribution and fitted it by Gaussian + pol2 , at high momentum were mass^2 distributions from different particles are overlapping we used the combination of two Gaussians + pol2. Fig.33 shows the mass^2 resolution for negative pions (blue points) and positive pions (red points) as a function of momentum. The momentum dependence of σ_{m^2} resolutions for (K^+, K^-) and (protons, $\bar{p}$) are presented in Fig.34 and Fig.35. The comparison shows that there is almost no difference in mass^2 resolution for positive and negative pions. However, the mass^2 resolution for negative particles were found to be better than for positive for pairs (K^+, K^-) and (protons, $\bar{p}$). The difference is more pronounced at low momentum, see Fig.34 and Fig.35. The low and high momentum ranges were pions, kaons and protons can be separated with 2.5 σ PID are presented in Fig.36-39 for positive and negative particles. The momentum range can be expaned by applying the cut on **Ecent** which improves the timing resolution of EMC.

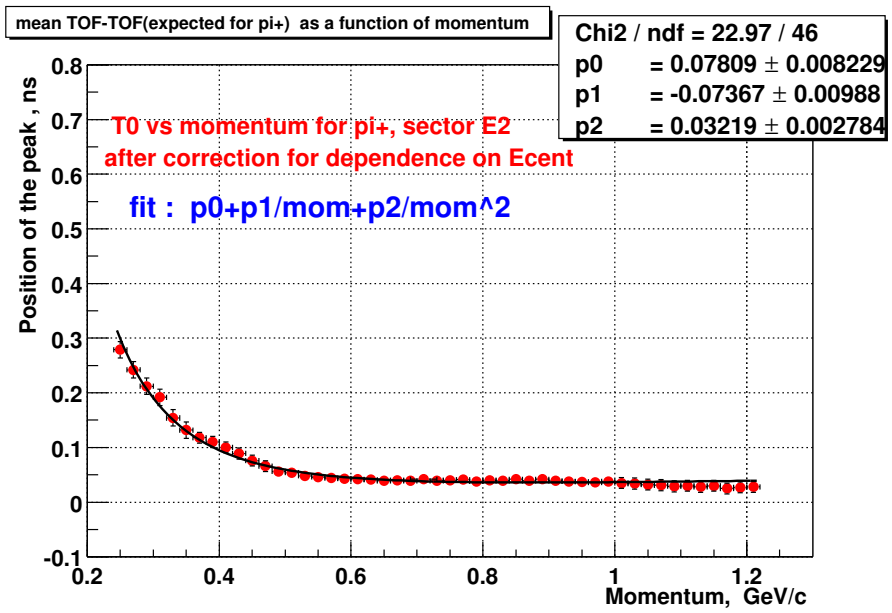

Figure 19: T0 offset (centroid of the difference temc-time(expected for π^+) as a function of momentum of π^+ detected in the sector E2, after removing the Ecent dependence of T0.

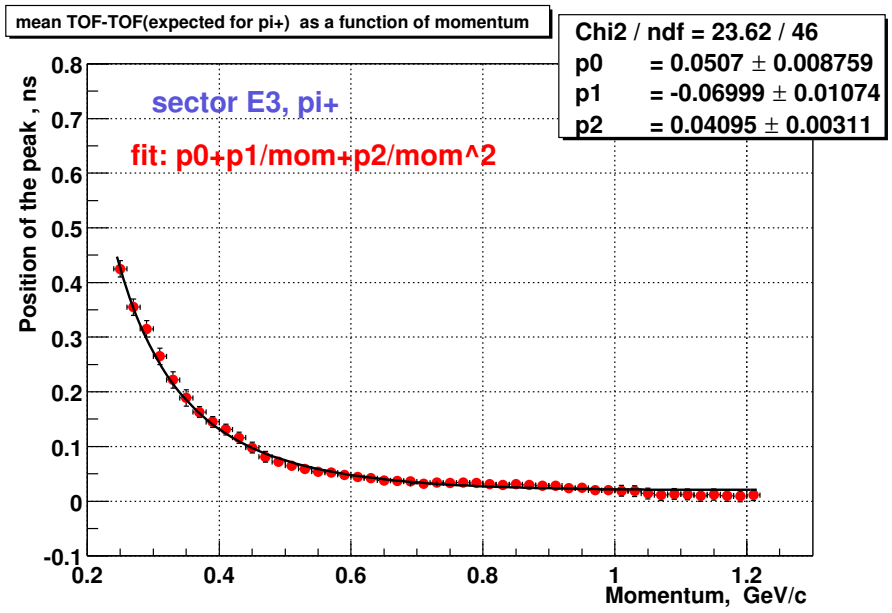

Figure 20: T0 offset (centroid of the difference temc-time(expected for π^+) as a function of momentum of π^+ detected in the sector E3, after removing the Ecent dependence of T0.

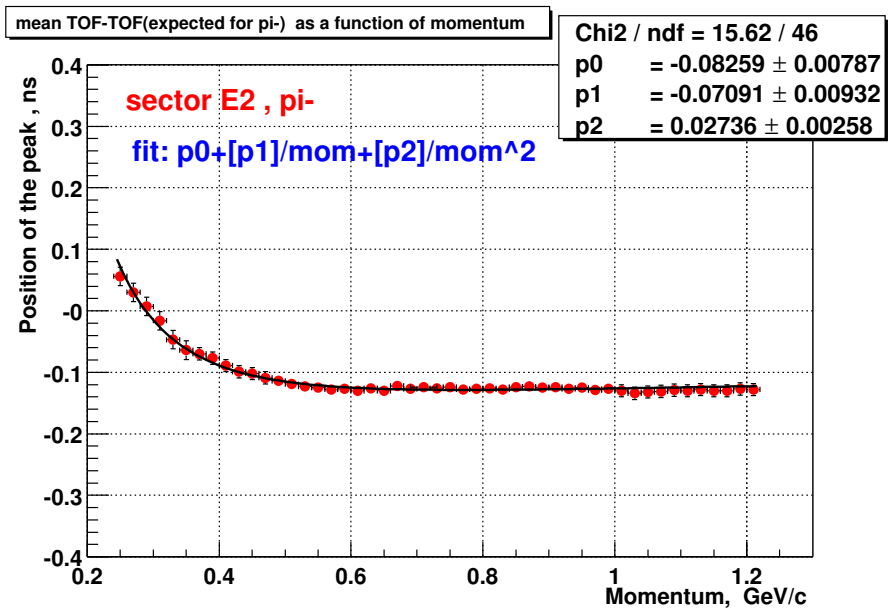

Figure 21: T0 offset (centroid of the difference temc-time(expected for π^-) as a function of momentum of π^- detected in the sector E2, after removing the Ecent dependence of T0.

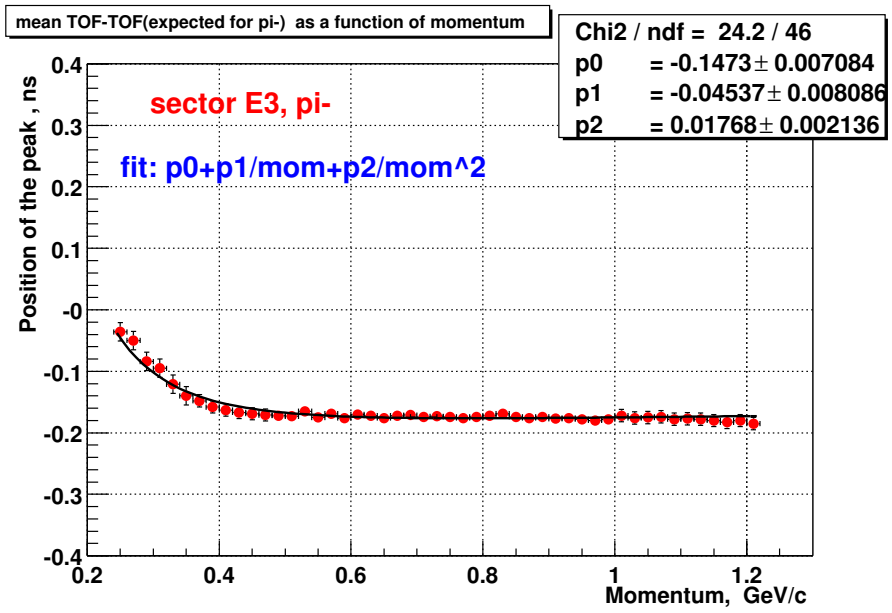

Figure 22: T0 offset (centroid of the difference temc-time(expected for π^-) as a function of momentum of π^- detected in the sector E3, after removing the Ecent dependence of T0.

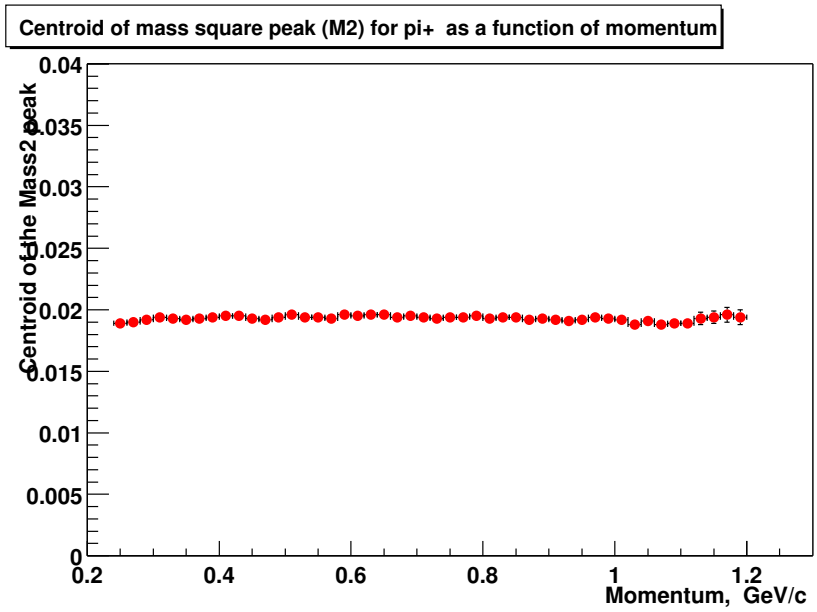

Figure 23: The position of mass^2 peak for positive pions as a function of momentum of π^+, after removing the Ecent-momentum dependence in T0 offset

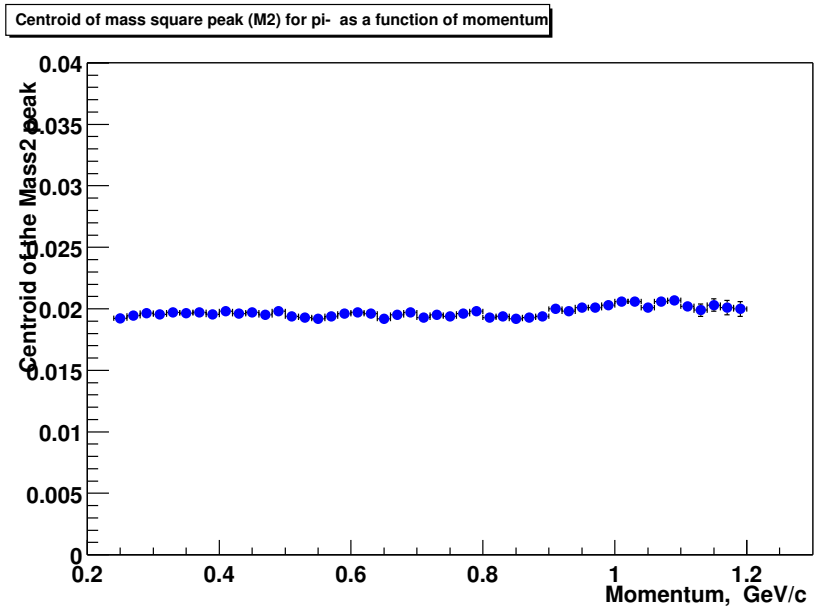

Figure 24: The position of mass^2 peak for negative pions as a function of momentum of π^-, after removing the Ecent-momentum dependence in T0 offset

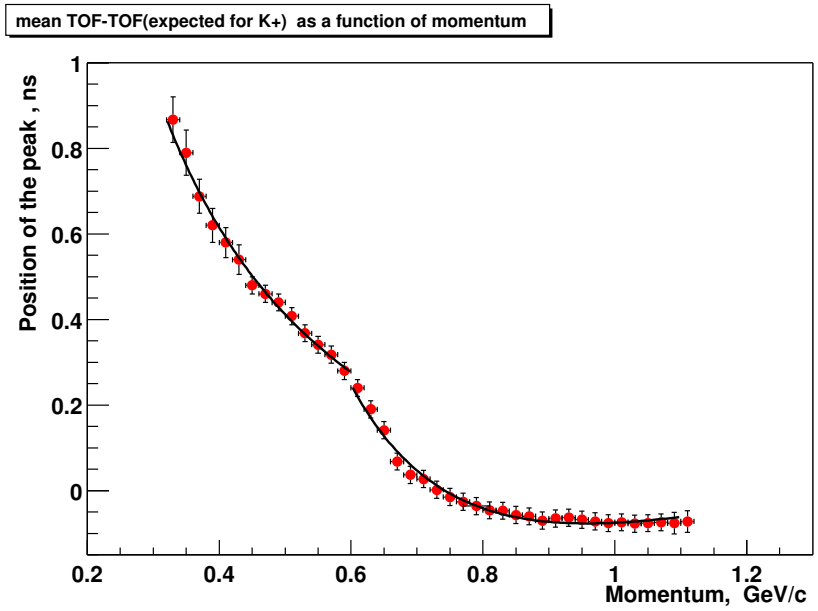

Figure 25: T0 offset (centroid of the difference temc-time(expected for K^+) as a function of momentum of K^+ mesons detected in the sector E2, after removing the Ecent dependence of T0.

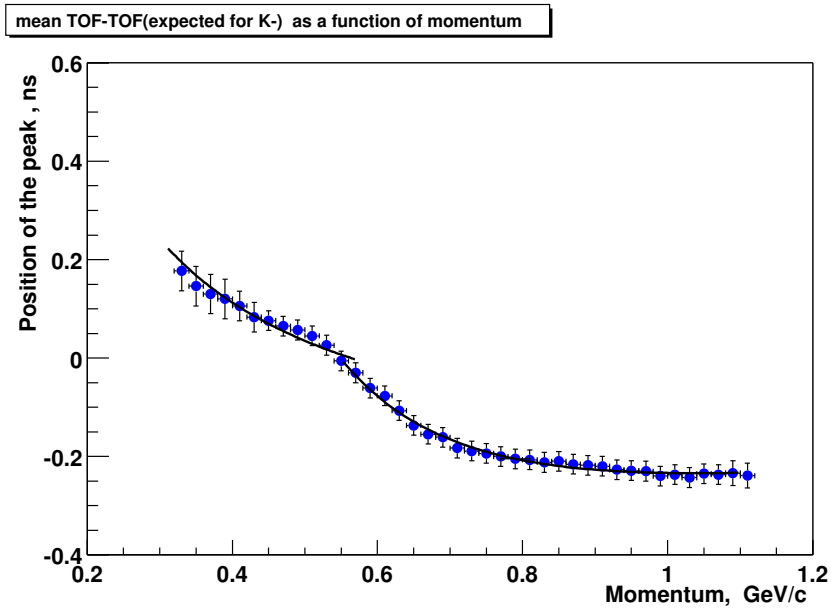

Figure 26: T0 offset (centroid of the difference temc-time(expected for K^-) as a function of momentum of K^- mesons detected in the sector E2, after removing the Ecent dependence of T0.

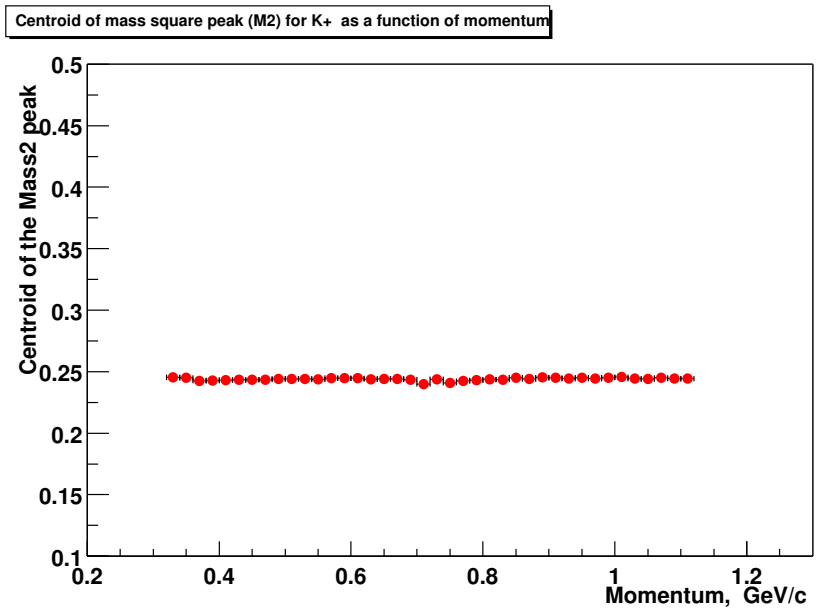

Figure 27: The position of mass^2 peak for positive kaons as a function of momentum of kaon after (Ecent, momentum) correction for T0 offset

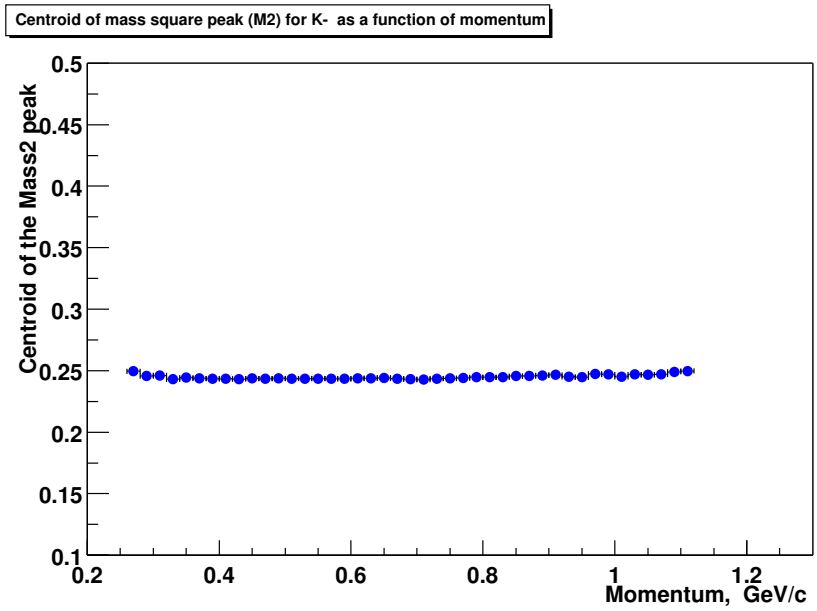

Figure 28: The position of mass^2 peak for negative kaons as a function of momentum of kaon after (Ecent, momentum) correction for T0 offset

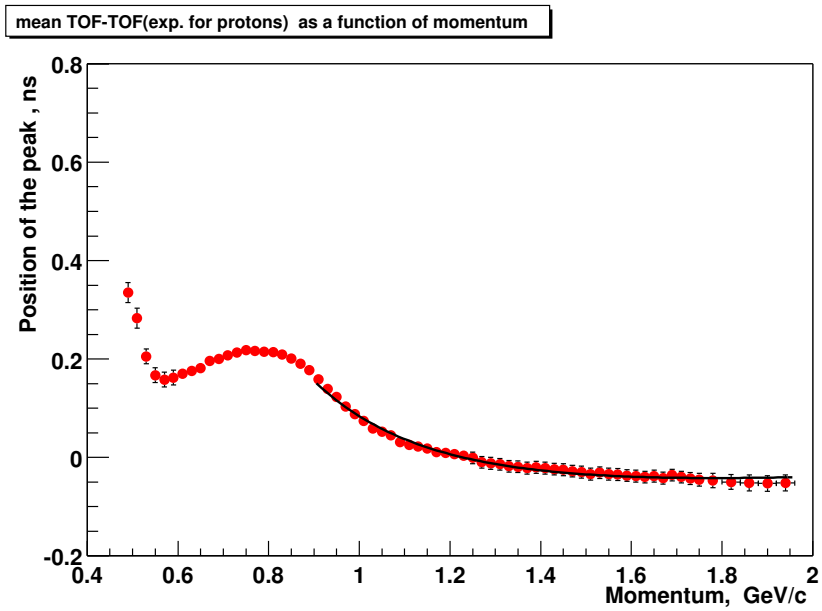

Figure 29: T0 offset (centroid of the difference temc-time(expected for proton) as a function of momentum of protons detected in the sector E2, after removing the Ecent dependence of T0.

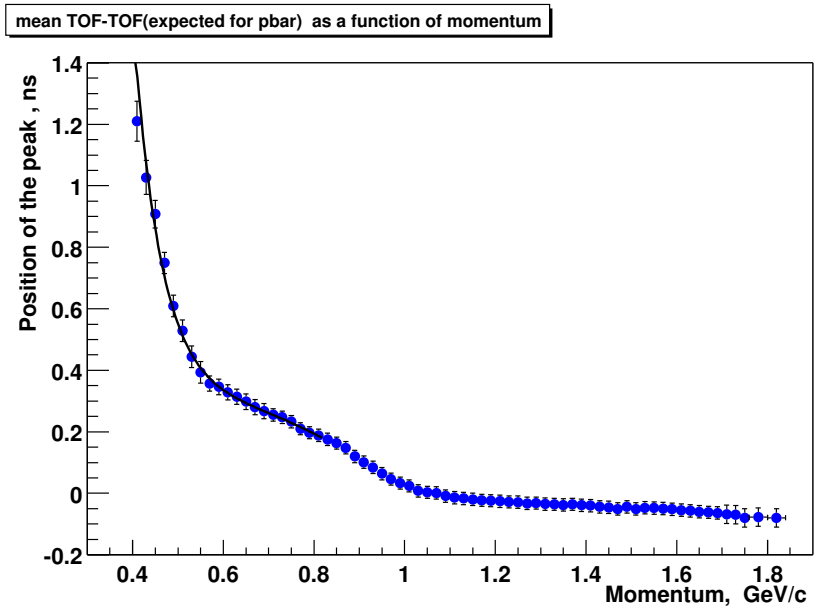

Figure 30: T0 offset (centroid of the difference temc-time(expected for $\bar{p}$) as a function of momentum of $\bar{p}$ detected in the sector E2, after removing the Ecent dependence of T0.

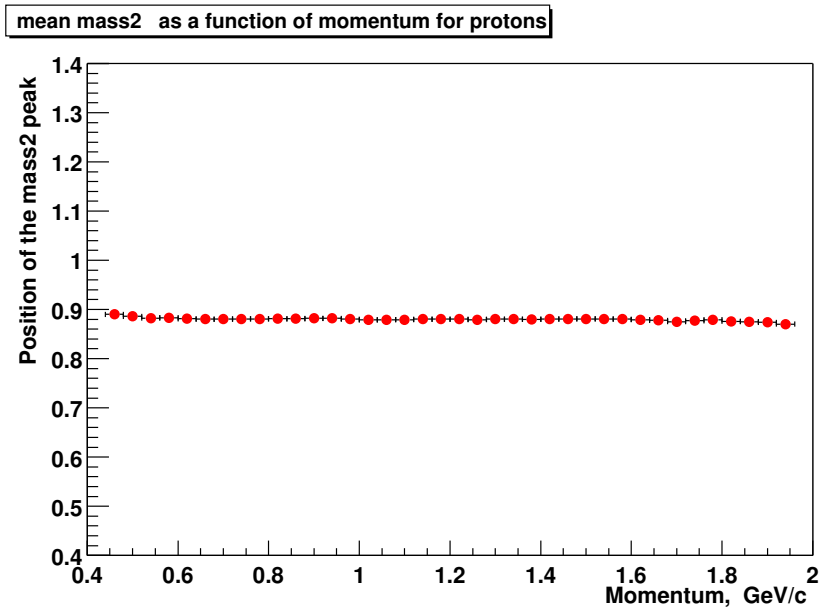

Figure 31: The position of mass^2 peak for protons as a function of momentum of proton after (Ecent, momentum) correction for T0 offset

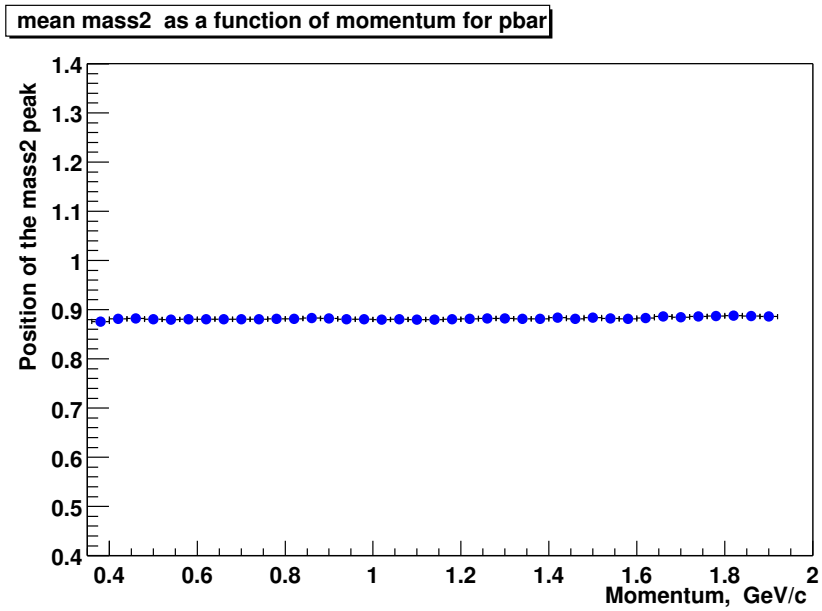

Figure 32: The position of mass^2 peak for $\bar{p}$ as a function of momentum of $\bar{p}$ after (Ecent, momentum) correction for T0 offset

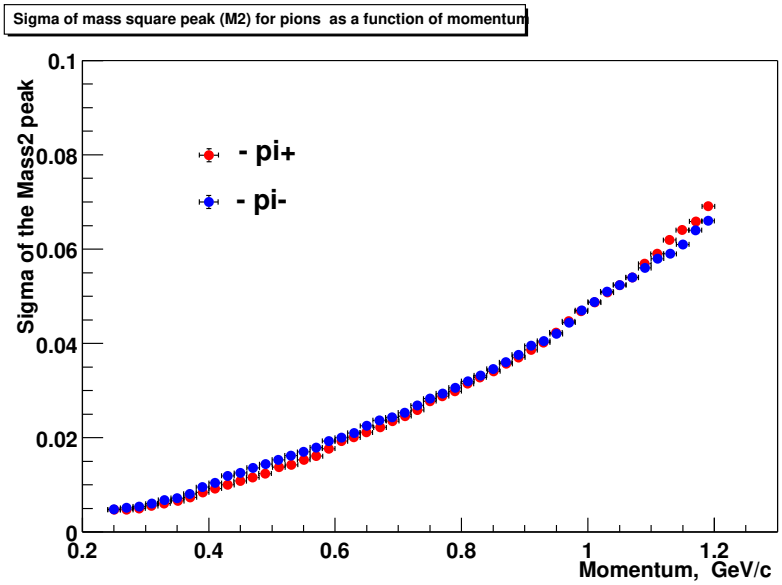

Figure 33: The mass^2 resolution for negative pions (blue points) and positive pions (red points) as a function of momentum.

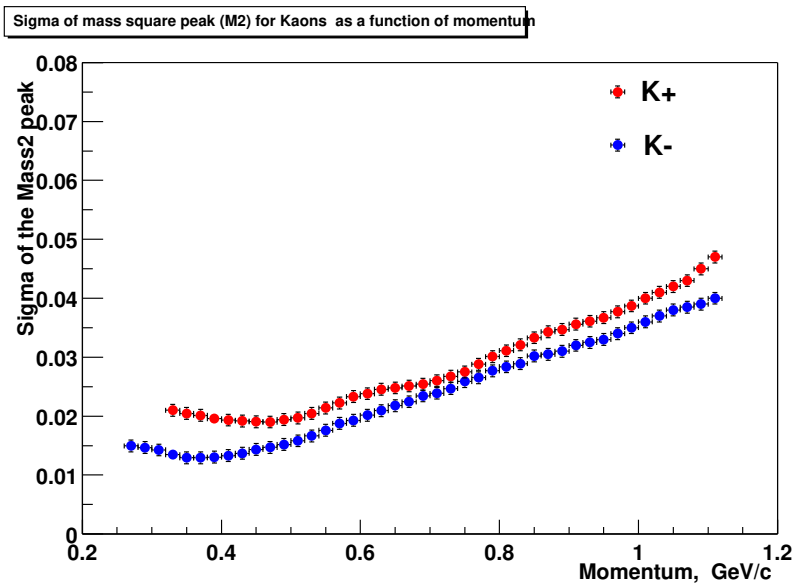

Figure 34: The mass^2 resolution for positive (red symbols) and negative (blue symbols) kaons as a function of momentum of kaon

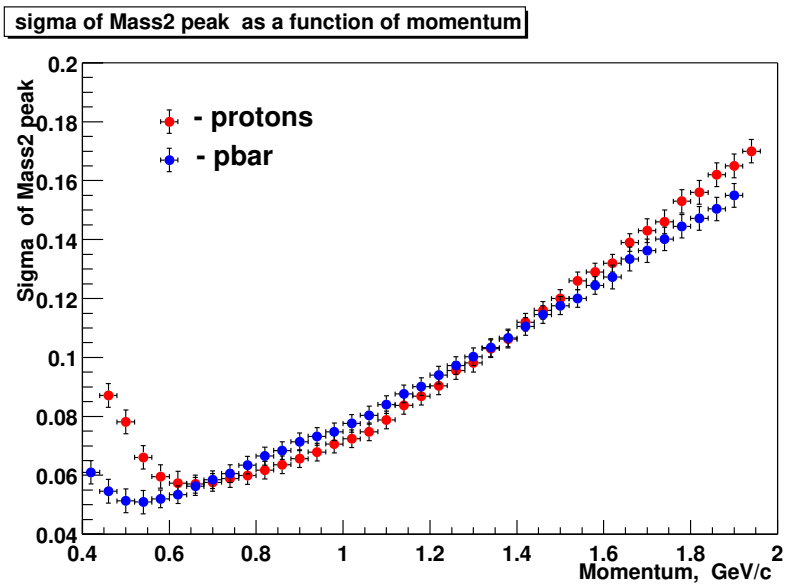

Figure 35: The mass^2 resolution for protons (red symbols) and $\bar{p}$ (blue symbols) as a function of momentum.

The code for T0 offset corrections and calculating PID functions: isPip (for π^+), isPim (for π^-), isKp (for K^+), isKm (for K^-), isPp (for protons) and isPm (for $\bar{p}$) will be posted into CVS: CVS: offline/analysis/run2hadron/hTree. It reads CNT nanoDSt's and creates Root Tree's which contain identified hadrons ($\pi^{\pm}$, p, $\bar{p}$) detected by East Arm PbSc (as the base the Y. Akiba method for nanoDST reading , see [1], was used). The all correction functions are located in the file hTree_corr.C.

References

[1] CVS:/offline/packages/CNT
T. K. Hemmick , F. Matathias, "nanoDST Users Guide"
http : *//www.phenix.bnl.gov/WWW/p/draft/felice/nanoguide*
T. K. Hemmick: CNT documentation:
https://www.phenix.bnl.gov/phenix/WWW/offline/CNT.html

[2] B. Jacak , QA Web page: *http* : *//www.phenix.bnl.gov/phenix/WWW/p/draft/jacak/qa/*

[3] J. Nagle "Documentation on EMC warnmap and deadmap"
https : *//www.phenix.bnl.gov/phenix/WWW/p/lists/phenix* − *e* − *l/msg*00311.*html*

[4] /phenix/data07/arkadij/offline/analysis/run2hadron/hTree

[5] T. Chujo et al., Phenix Analysis Note AN 024
" Determination of of Charged Hadron PID boundaries by TOF"
R. Averbeck et al, Phenix Analysis Note AN 037
" Particle Identification by Correlating Time-of-flight and Momentum Measurement"

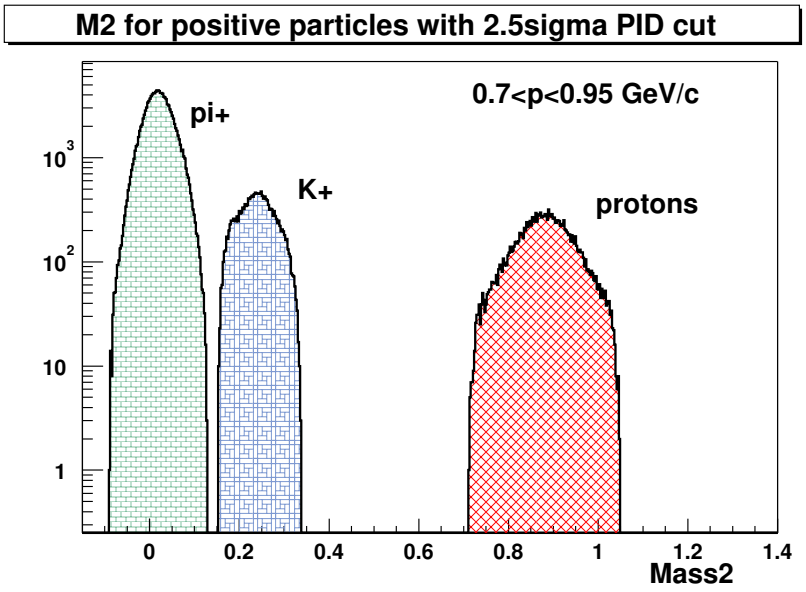

Figure 36: The mass-squared mass^2 for positive particles after applying 2.5 σ PID cut, the momentum range is 0.7≤p≤0.95 GeV/c

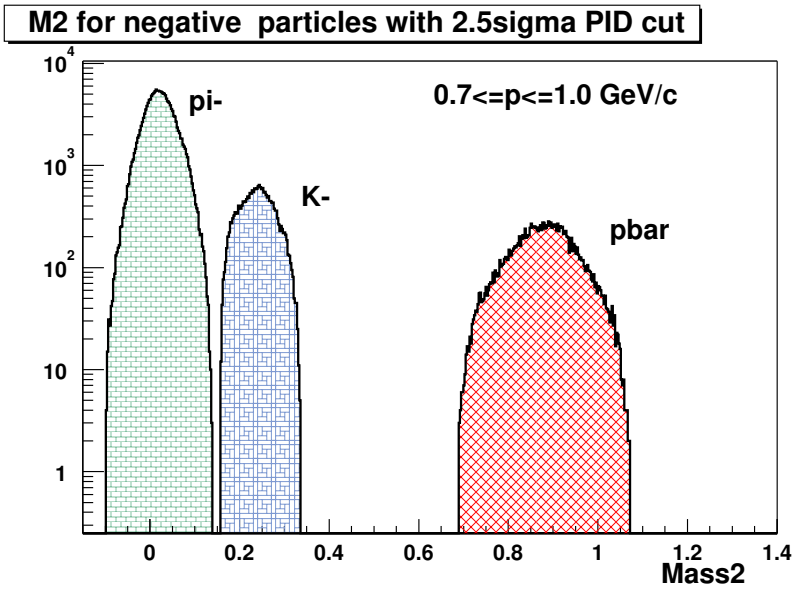

Figure 37: The mass-squared mass^2 for negative particles after applying 2.5 σ PID cut, the momentum range is 0.7≤p≤1.0 GeV/c

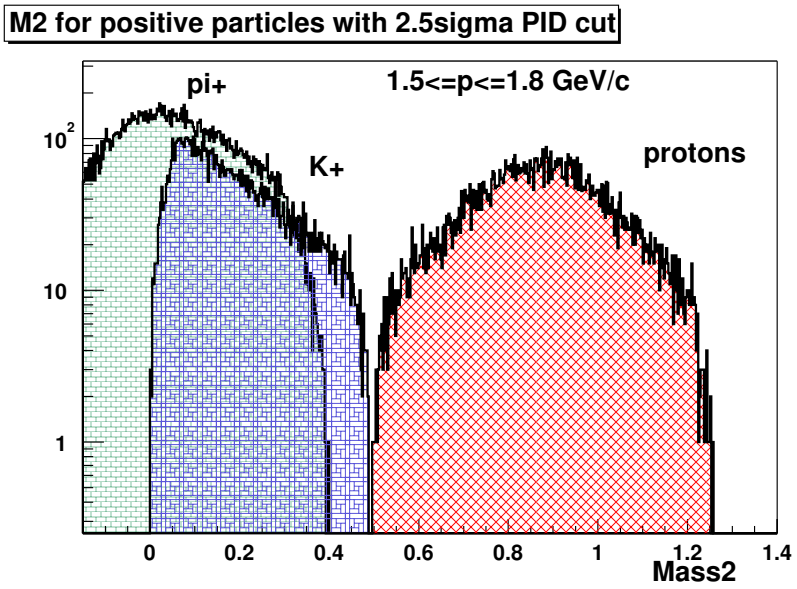

Figure 38: The mass-squared mass^2 for positive particles after applying 2.5 σ PID cut, the momentum range is 1.5≤p≤1.8 GeV/c

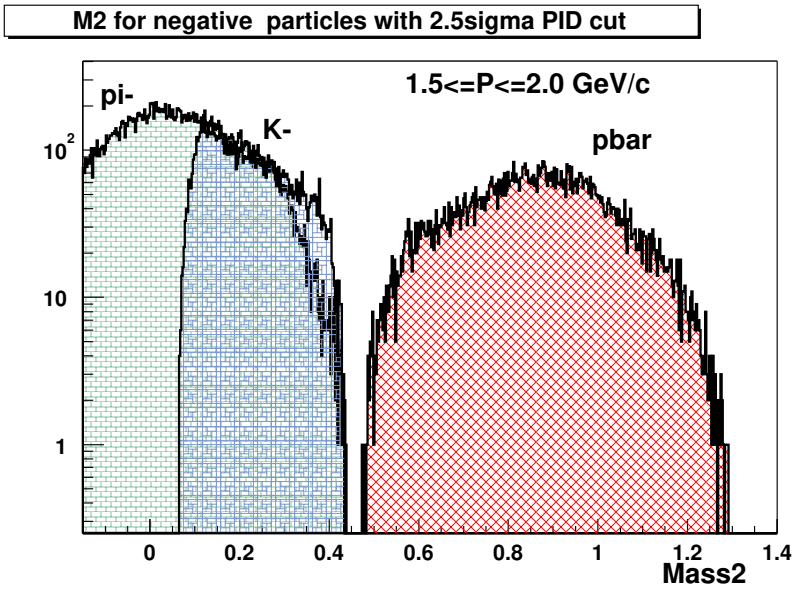

Figure 39: The mass-squared mass^2 for negative particles after applying 2.5 σ PID cut, the momentum range is 1.5≤p≤2.0 GeV/c

[6] J. Burward-Hoy et al. Phenix Analysis Note AN172
"Measuring the momentum resolution using TOF and Drift Chamber"
https://www.phenix.bnl.gov/WWW/p/draft/purwar/momres.ps

[7] utiHadPiD Library: CVS:/offline/packages/uti/utiHadPid(*.cc,*.hh)

[8] T.Chujo "Systematic of TOF resolution", Analysis meeting 17/04/2002
https://www.phenix.bnl.gov/WWW/p/draft/chujo/anameeting_apr17_02
T.Chujo "TOF Global Time Zero Afterburner", Analysis meeting 22/05/2002
https://www.phenix.bnl.gov/WWW/p/draft/chujo/anameeting_may22_02

[9] Electromagnetic Calorimeter: Conceptual Design Report, 1993
https : //www.phenix.bnl.gov/phenix/WWW/emcal/project_doc/cdr.html

[10] T. Nyak, B. Zajc, B. Cole, Hadron Physics in Phenix , Phenix note pn66 , 1992
http : //www.nevis.columbia.edu/phenix/physics/hadrons/notes/notes.html

[11] G. David et al, "The Phenix PbSc Calorimeter and its Performance", proceedings of CALOR97
https://www.phenix.bnl.gov:8080/phenix/WWW/emcal/papertrail/calor97.ps

[12] M. Chiu et al. (EMC group), EMCal calibration in preparation for QM2002
Phenix technical note tn400, 2002-17-12

[13] P. Tarjan: EMC ToF corrections for run2 v03
http://www.phenix.bnl.gov/WWW/p/draft/ptarjan/EmcTofAfterBurner/

[14] S. Mioduszewski, "Energy dependent shifts in timing peak"
http://www.phenix.bnl.gov/WWW/p/draft/saskia/afterburner/TimingShiftvsE.PDF
https://www.phenix.bnl.gov/phenix/WWW/p/draft/saskia/afterburner/TimingShiftEMCal.PDF

[15] G. David , private communication, 2003

[16] eTree package: CVS:/offline/analysis/run2electron/eTree